Abdominal Imaging

Received: 23 July 2003 / Revision accepted: 17 Dec. 2003 / Published online: 12 May 2004

Abdom Imaging (2004) 29:467–471
DOI: 10.1007/s00261-004-0177-4

Hemodynamics of intrahepatic cholangiocarcinoma: Evaluation with single-level dynamic CT during hepatic arteriography

F. Miura,* S. Okazumi, W. Takayama, T. Asano, H. Makino, K. Shuto, T. Ochiai

Department of Academic Surgery, Graduate School of Medicine, Chiba University, Chiba, Japan

Abstract

Background: We determined the radiologic characteristics of intrahepatic cholangicarcinoma (ICC) on single-level dynamic computed tomography during hepatic arteriography (CTHA) and assessed the hemodynamics of the tumor.
Methods: Eleven patients with pathologically confirmed ICC underwent single-level dynamic CTHA. After placing the catheter tip in the proper hepatic artery and running a 30-s continuous scan, scanning was performed every 15 or 30 s for 120 s. The change of contrast-enhancement pattern of the ICCs were interpreted retrospectively.
Results: The pattern of enhancement was classified into two types: vascular and hypovascular. In the vascular type, the contrast enhancement gradually spread from each intratum oral artery and became mottled. It changed from a mottled and hypoattenuated pattern to an even and hyperattenuated appearance in comparison with the adjacent liver approximately 120 s after the injection of contrast agent. In the hypovascular type, the tumor was barely enhanced and remained hypoattenuated compared with the adjacent liver at 120 s after the beginning of the injection. The 11 ICCs were classified into eight vascular types and three hypovascular types. Intratumoral arteries were visualized in nine tumors: eight vascular types and one hypovascular type.
Conclusion: The contrast-enhancement pattern of ICC on single-level dynamic CTHA is related to the intratumoral artery.

Key words: Liver neoplasms—Computed tomography—Angiography—Intrahepatic cholangiocarcinoma

Intrahepatic cholangiocarcinoma (ICC) is a primary adenocarcinoma of the liver that arises from the epithelial cells of the intrahepatic bile ducts, specifically a segmental or more peripheral duct, and presents as a focal liver mass [1], in contrast to hilar cholangiocarcinoma (Klatskin tumor) [2], which originates from hepatic ducts. After hepatocellular carcinoma (HCC), it is the second most common primary hepatic malignant tumor and accounts for 10% of primary liver cancers [3].

On contrast-enhanced computed tomography (CT), ICC has been depicted as an irregular mass of markedly low attenuation with contrast enhancement at the tumor periphery durng hepatic arterial and portal venous phases [4]. This pattern differs from that associated with hypervascular tumors such as HCC, which most commonly have predominatly high attenuation during the hepatic arterial phase and isoattenuation or low attenuation during the portal venous phase [4]. Imaging modalities such as CT during arterial portography (CTAP) [5, 6], CT during hepatic arteriography (CTHA) [7, 8], dynamic magnetic resonance imaging (MRI) [9], and Doppler ultrasound [10] have facilitated investigation of the hemodynamics of liver tumors. In particular, single-level dynamic CTHA, a new method of delineating the blood flow in hepatic tumors, has been used to elucidate the hemodynamics of HCC [11, 12], but, although the CT features of ICC have been described [13, 14], to our knowledge, its appearance on single-level dynamic CTHA has not been described. Therefore, we investigated the radiologic characteristics of ICC on single-level dynamic CTHA and assessed its hemodynamics.

Materials and methods

Between December 1995 and March 2002, 18 consecutive patients with suspected ICC on CT, MRI, or sonography were referred for investigation, and single-level dynamic CTHA was carried out in 12 (four patients did not undergo imaging because they had undergone angiography at a previous hospital, and the other two patients had a prolonged series of examinations that included angiography, CTAP,

Present address: Department of Surgery, Teikyo University, School of Medicine, 2-11-1, Kaga, Itabashi-ku, Tokyo, 173-8605, Japan

Correspondence to: F. Miura; *email:* f-miura@med.teikyo-u.ac.jp

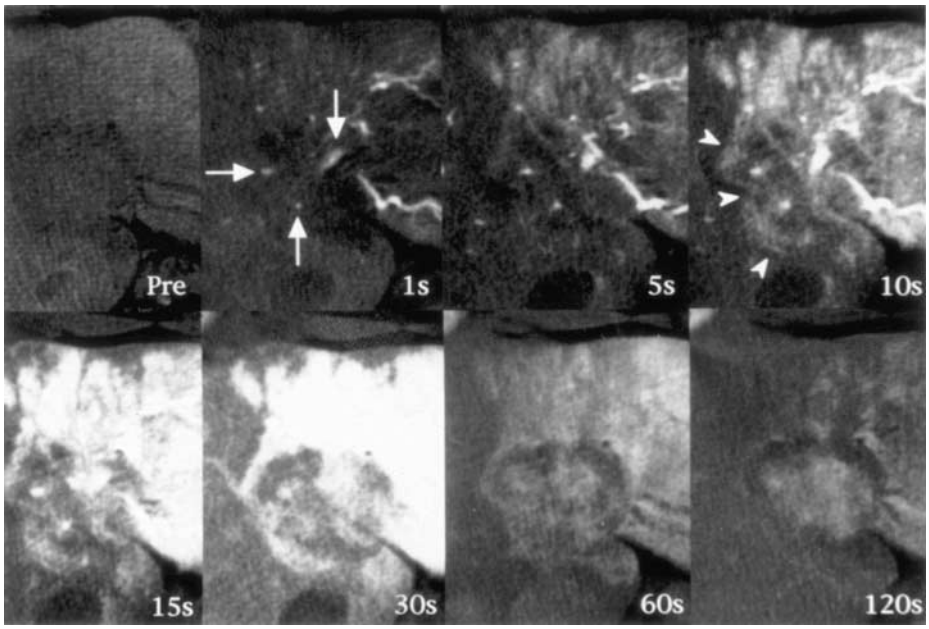

Fig. 1. Vascular type. A 46-year-old man with intrahepatic cholangiocarcinoma in the left lobe. Single-level dynamic CTHA images obtained before intraarterial injection of contrast (Pre) and 1, 5, 10, 15, 30, 60, and 120 s after injection of contrast. Intratumoral arteries (*arrows*) are clearly seen at 1 s. At 5 s, a segmental staining begins to be enhanced. At 10 s, peripheral enhancement (*arrowheads*) appears. Peripheral enhancement mimics the enhancement pattern and overlaps segmental staining. The tumor enhancement spreads from each intratumoral artery and becomes mottled at 30 s. At 120 s, tumor enhancement becomes even and hyperattenuated.

and conventional CTHA). One of the 12 patients was excluded from the evaluation because of incorrect breath-holding during scanning. Therefore, 11 patients (eight men, three women; age range, 45–72 years; mean age; 60.1 years) formed the study population and all gave informed consent. All 11 tumors (diameter, 2–6 cm; mean, 4.3 cm) had been detected on conventional CTHA performed immediately before single-level dynamic CTHA, and all were classified as the mass-forming type according to the classification of primary liver cancer proposed by the Liver Cancer Study Group of Japan, which defines mass-forming type tumors as a nodular tumor in the liver parenchyma that has originated from peripheral bile ducts. The tumor was located in the right lobe in six patients and in the left lobe in five patients. After the single-level dynamic CTHA examination, 10 patients underwent laparotomy: eight had the tumor surgically resected, and two tumors were inoperable because of peritoneal dissemination. The pathologic diagnosis of ICC was obtained from the resected specimen (eight patients), intraoperative biopsy (two patients), or percutaneous needle biopsy (one patient).

Angiography, unenhanced CT, CTAP, and conventional CTHA were performed before single-level dynamic CTHA, as was celiac and superior mesenteric angiography for evaluation of the arterial anatomy. The single-level dynamic CTHA examination took place more than 10 min after conventional CTHA, the findings of which were used to determine the most suitable craniocaudal level that ensured that the axial plane including the maximal cross-sectional diameter of the tumor would be scanned. After placing a 5-F angiographic catheter tip into the proper hepatic artery under fluorosopic guidance, iopamidol (Iopamiron 300, Schering, Berlin, Germany) was diluted with saline to 100 mg/mL. Sixty milliliters of the solution was injected at a rate of 3 mL/s by using a power injector. Scans were obtained with helical CT (Somaton Plus-4, Siemens Medical Systems, Erlangen, Germany) or multidetector CT (Aquilion, Toshiba, Tokyo, Japan). Scanning was started immediately after the injection of contrast medium; during a single breath-hold, a 30-s continuous scan was obtained with 5-mm collimation, 1-s scan time, 2-s interscan time, 280 mAs, 120 kVp, and 512 × 512 matrix for the Somaton Plus-4 or 5-mm collimation, 0.5-s scan time, 0.5-s interscan time, 300 mAs, 120 kVp, and 512 × 512 matrix for the Aquilion. After the continuous scan, scans were obtained every 15 or 30 s for 120 s. Oxygen was administered to patients during the imaging procedure. The CT image of every scan was documented on laser film.

Retrospective interpretation of the CT images was established by consensus between two observers. The change of contrast-enhancement pattern of ICC on the single-level dynamic CTHA images were interpreted visually, as were recording the time to appearance of an intratumoral artery and peripheral enhancement.

Results

Single-level dynamic CTHA demonstrated the hemodynamics of all tumors, and the contrast-enhancement patterns were classified into two types, vascular and hypovascular, each of which had a distinctive time course. In the vascular type (Fig. 1), at 1 to 5 s (mean, 2.75 s) after the injection of

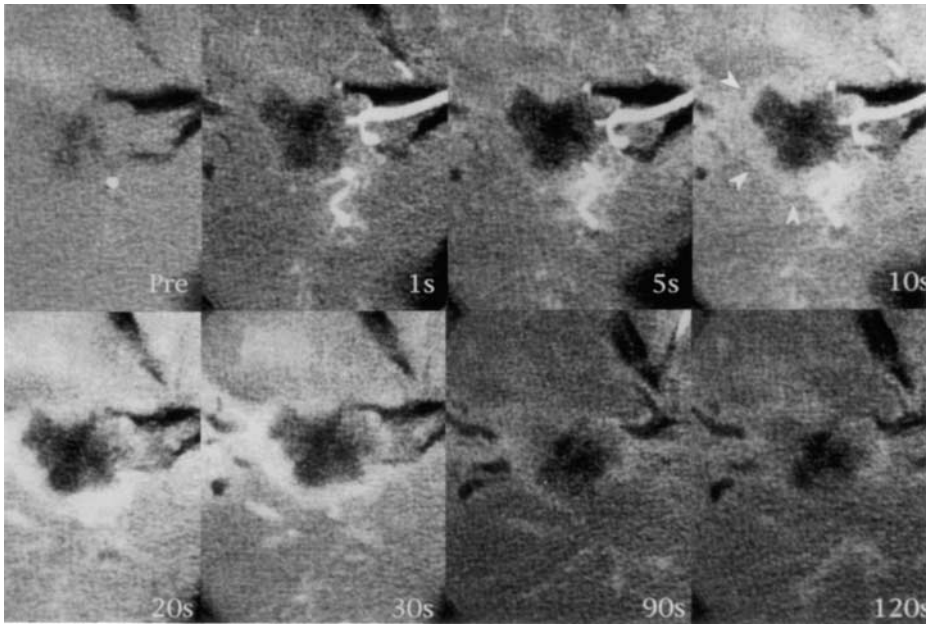

Fig. 2. Hypovascular type. A 60-year-old man with intrahepatic cholangiocarcinoma in the right lobe. Single-level dynamic CTHA images obtained before intraarterial injection of contrast (Pre) and 1, 5, 10, 20, 30, 90, and 120 s after injection of contrast. The tumor is barely enhanced and still hypoattenuated compared with the adjacent liver 120 s after the beginning of the injection. Peripheral enhancement (*arrowheads*) begins to appear at 10 s and lasts until 120 s.

contrast, intratumoral arteries were seen immediately and clearly. Contrast enhancement of the adjacent liver appeared 5 to 12 s (mean, 8.0 s) after the beginning of the injection, and peripheral enhancement began almost simultaneously. The contrast enhancement gradually spread from each intratumoral artery and became mottled for approximately 30 s after the beginning of the injection. Enhancement of the adjacent liver disappeared, but that of the tumor did not and instead changed from a mottled and hypoattenuated pattern to an even and hyperattenuated appearance in comparison with the adjacent liver approximately 120 s after the beginning of the injection. In the hypovascular type (Fig. 2), contrast enhancement of the adjacent liver appeared 6 to 12 s (mean, 9.7 s) after the beginning of the injection of contrast, but the tumor was barely enhanced and remained hypoattenuated when compared with the adjacent liver at 120 s after the beginning of the injection. Of the 11 ICCs, eight were classified as vascular and three as hypovascular. All eight vascular tumors had the mottled hyperattenuated pattern of enhancement until approximately 1.5 min after the injection of contrast, when four became evenly hyperattenuated.

Intratumoral arteries were visualized in nine tumors: all eight vascular type tumors and one hypovascular type. In seven vascular tumors, the enhancement spread from the intratumoral artery; however, in the hypovascular type of tumor, the intratumoral artery was only faintly visualized and the contrast enhancement barely spread from it.

Peripheral enhancement, i.e., thin mild incomplete rim-like enhancement surrounding the tumor, was seen in eight cases (six vascular and two hypovascular) and started to appear 5 to 12 s (average, 9.2 s) after the injection of contrast material. In four vascular-type tumors scanned by multidetector CT, arteries were seen at the tumor periphery immediately after the injection of contrast (Fig. 3), and the enhancement spread from each artery, resulting in peripheral enhancement. Segmental stainings, wedge-shape segmental hyperattenuated areas extending from the hepatic hilus to the surface, or segmental boundaries of the liver were seen in 10 of 11 (90.1%) patients, until approximately 2 min after the injection of contrast, and they mimicked the enhancement pattern and overlapped the peripheral enhancement (Figs. 1, 3).

Discussion

Previous reports of the radiologic findings of ICC on conventional dynamic CT and dynamic MRI have shown that the tumor usually appears as an avascular mass, a rounded nonencapsulated hypodense mass with irregular margins, and with delayed contrast enhancement [3, 13–15]. Those imaging modalities have limitations in demonstrating the hemodynamics of ICC in detail, so the actual time course of the contrast enhancement of the tumor has not been established. Differential diagnosis of ICC from other liver tumors is important because its rate of lymph node metastasis is high and lymph node dissection is essential [16, 17]. However, even at biopsy, the histopathologic diagnosis of ICC is difficult and requires reasonable exclusion of other adenocarcinomas that may have metastasized to the liver [18]. To date, single-level dynamic CTHA has not been used extensively for evaluation of ICC because it is an uncommon tumor; we have been using conventional CTHA for the differential diagnosis of ICC since November 1994, and in the present study we reviewed our findings of the hemodynamics and the radiologic characteristics of this tumor.

The blood supply to liver neoplasms such as HCC, cavernous hemangioma, and colorectal metastasis is mainly through the hepatic artery [19, 20], and intratumoral arteries

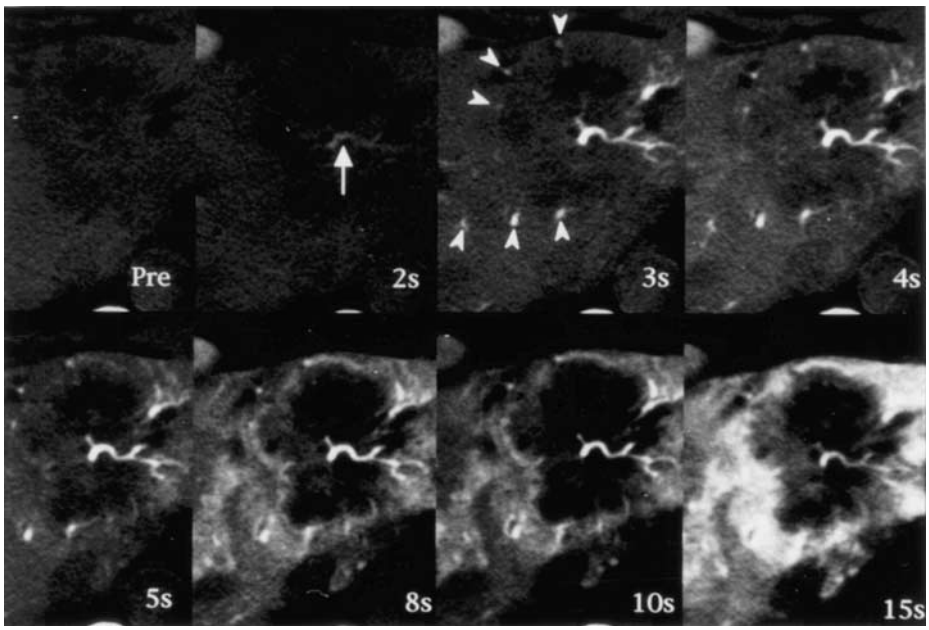

Fig. 3. A 57-year-old man with intrahepatic cholangiocarcinoma in the left lobe. Single-level dynamic CTHA images obtained before intraarterial injection of contrast (Pre) and 2, 3, 4, 5, 8, 10, and 15 s after injection of contrast. Intratumoral arteries (*arrow*) are clearly seen at 2 s. At 3 s, arteries (*arrowheads*) can be seen in the tumor periphery. The enhancement diffused from each artery and resulted in peripheral enhancement at 10 s, which mimics the enhancement pattern and overlaps segmental staining.

are frequently seen in hypervascular tumors, such as HCC, and in focal nodular hyperplasia [11, 21]. However, there have been few reports of intratumoral arteries of ICC being demonstrated on CT. In the present study, intratumoral arteries were identified immediately after the injection of contrast, which affected the vasucularity of the ICC. Although there have been few reports about the clinical utility of arterial chemoinfusion therapy in ICC [22], our results suggests the feasibility of arterial chemoinfusion therapy for ICC. A mottled pattern of contrast enhancement has been reported as a characteristic appearance of ICC [23], although how it occurred was not described. Our results suggest that tumor enhancement gradually spreads from each intratumoral artery thus producing the mottled appearance. We consider that the intratumoral arteries are hepatic arteries encased by the tumor or neovascularities; however, determination of the origin of the intratumoral artery of ICC will require further study.

HCC and colorectal liver metastases frequently show rim enhancement on CTHA, and Ueda et al. suggested that it reflects a drainage area [11], whereas Irie et al. believed that the rim enhancement of liver metastasis on CTHA corresponds to compressed liver parenchyma around the metastasis because it would not have a portal blood supply and would compensate for this by increasing the arterial blood supply [24]. As for the peripheral enhancement seen in ICC, it is thought to be a relative hypervascularity [25, 26]. In the present series, four vascular-type tumors that were scanned by multidetector CT had arteries detected in the periphery of the tumor immediately after injection of the contrast, and the contrast enhancement spread from each artery, resulting in a peripheral enhancement. There were also tumors in which peripheral enhancement mimicked the enhancement pattern and overlapped sgmental stainings. Because hepatic arterial flow increases to compensate for the decrease in portal venous flow, caused by the narrowing or obstruction of the portal vein from invasion or extrinsic compression by the tumor, dynamic CT and CTHA can depict these areas of segmental stainings that correspond to areas of low attenuation on CTAP [27, 28]. It is assumed that the most of the increased enhancement is a functional change resulting from increased perfusion because the pathologic changes in liver cells in these areas have been slight in most cases [29, 30]. We believe these findings corroborate that the peripheral enhancement of ICC is caused by a relative hypervascularity in the tumor periphery. In other words, we speculate that peripheral enhancement of ICC does not correspond to the area of tumor cells but of the liver parenchyma. We recognize that the number of patients in this study is small, and we know that markedly hypervascular ICCs have been reported [31]; therefore, further investigations are needed before drawing conclusions.

In summary, single-level dynamic CTHA is useful for evaluating the hemodynamics of ICC. We believe that the blood supply for this tumor is the hepatic artery and that the enhancement pattern is related to the intratumoral artery. Further, we presume the peripheral contrast enhancement of ICC is caused by a relative hypervascularity in the tumor periphery.

References

1. Liver Cancer Group of Japan (1998) Classification of primary liver cancer, 1st English ed. Kanehara, Tokyo, pp 6–7
2. Klatskin G (1965) Adenocarcinoma of the hepatic duct at its bifurcation within the porta hepatis. Am J Med 34:241–256
3. Craig JR, Peters RL, Edmondson HA (1989) Tumors of the liver and intrahepatic bile ducts: atlas of tumor pathology, 2nd series, fasc 26. Armed Forces Institute of Pathology, Washington, DC, pp 197–221
4. Loyer EM, Chin H, DuBrow RA, et al. (1999) Hepatocellular carcinoma and intrahepatic peripheral cholangiocarcinoma: enhancement

patterns with quadruple phase helical CT—a comparative study. Radiology 212:866–875
5. Matsui O, Kadoya M, Suzuki M, et al. (1983) Work in progress: dynamic sequential computed tomography during arterial portography in the detection of hepatic neoplasms. Radiology 146:721–727
6. Matsui O, Kadoya M, Kameyama T, et al. (1991) Benign and malignant nodules in cirrhotic livers: distinction based on blood supply. Radiology 178:493–497
7. Prando A, Wallace S, Bernardino ME, et al. (1979) Computed tomographic arteriography of the liver. Radiology 130:697–701
8. Takayasu K, Muramatsu Y, Moriyama N, et al. (1992) Focal nodular hyperplasia of the liver: arterial angio-CT and microangiography. J Comput Assist Tomogr 16:212–215
9. Ohtomo K, Itai Y, Yoshikawa K, et al. (1987) Hepatic tumors: dynamic MR imaging. Radiology 163:27–31
10. Tanaka S, Kitamura T, Fujita M, et al. (1990) Color Doppler flow imaging of liver tumors. AJR 154:509–514
11. Ueda K, Matsui O, Kawamori Y, et al. (1998) Hypervascular hepatocellular carcinoma: evaluation of hemodynamics with dynamic CT during hepatic arteriography. Radiology 206:161–166
12. Ueda K, Matsui O, Kawamori Y, et al. (1998) Differentiation of hypervascular hepatic pseudolesions from hepatocellular carcinoma: value of single-level dynamic CT during hepatic arteriography. J Comput Assist Tomogr 22:703–708
13. Ros PR, Buck JL, Goodman ZD, et al. (1988) Intrahepatic cholangiocarcinoma: radiologic–pathologic correlation. Radiology 167:689–693
14. Kim TK, Choi BI, Han JK, et al. (1997) Peripheral cholangiocarcinoma of the liver: two-phase spiral CT findings. Radiology 204:539–543
15. Soyer P, Bluemke DA, Reichle R, et al. (1995) Imaging of intrahepatic cholangiocarcinoma. 1: Peripheral cholangiocarcinoma. AJR 165:1427–1431
16. Isaji S, Kawarada Y, Taoka H, et al. (1999) Clinicopathological features and outcome of hepatic resection for intrahepatic cholangiocarcinoma in Japan. J. Hepatobiliary Pancreat Surg 6:108–116
17. Kawarada Y, Mizumoto R (1990) Diagnosis and treatment of cholangiocellular carcinoma of the liver. Hepatogastroenterology 37:176–181
18. Lee RG (1994) Diagnostic liver pathology. Mosby, St. Louis, pp 457–461
19. Bierman HR, Byron RL, Kelley KH (1951) Studies on the blood supply of tumors in man. III: Vascular patterns of the liver by hepatic arteriography in vivo. J Natl Cancer Inst 12:107–131
20. Nakashima T (1975) Vascular changes and hemodynamics in hepatocellular carcinoma. In: Okuda K, Peter RL (eds) Hepatocellular carcinoma. Wiley, New York, pp 169–203
21. Miyayama S, Matsui O, Ueda K, et al. (2000) Hemodynamics of small hepatic focal nodular hyperplasia: evaluation with single-level dynamic CT during hepatic arteriography. AJR 174:1567–1569
22. Tanaka N, Yamakado K, Nakatsuka A, et al. (2002) Arterial chemoinfusion therapy through an implanted port system for patients with unresectable intrahepatic cholangiocarcinoma-initial experience. Eur J Radiol 41:42–48
23. Lacomis JM, Baron RL, Oliver JH III, et al. (1997) Cholangiocarcinoma: delayed CT contrast enhancement patterns. Radiology 203:98–104
24. Irie T, Tsushima Y, Terahata S, et al. (1997) Rim enhancement in colorectal metastases at CT during infusion hepatic arteriography: does it represent liver parenchyma or live tumor cell zone. Acta Radiol 38:416–421
25. Zhang Y, Uchida M, Abe T, et al. (1999) Intrahepatic peripheral cholangiocarcinoma: comparison of dynamic CT and dynamic MRI. J Comput Assist Tomogr 23:670–677
26. Takayasu K, Ikeya S, Mukai K, et al. (1990) CT of hilar cholangiocarcinoma: late contrast enhancement in six patients. AJR 154:1203–1206
27. Itai Y, Moss AA, Goldberg HI (1982) Transient attenuation difference of lobar or segmental distribution detected by dynamic computed tomography. Radiology 143:719–726
28. Freeny PC, Marks WM (1986) Hepatic perfusion abnormalities during CT angiography: detection and interpretation. Radiology 159:685–691
29. Yamashita Y, Takahashi M, Kanazawa S, et al. (1992) Parenchymal changes of the liver in cholangiocarcinoma: CT evaluation. Gastrointest Radiol 17:161–166
30. Nagino M, Nimura Y, Kamiya J, et al. (1998) Immediate increase in arterial blood flow in embolized hepatic segments after portal vein embolization: CT demonstration. AJR 171:1037–1039
31. Yoshida Y, Imai Y, Murakami T, et al. (1999) Intrahepatic cholangiocarcinoma with marked hypervascularity. Abdom Imaging 24:66–68